



HAL
open science

Effect of trace metal-limited growth on the postmortem dissolution of the marine diatom *Pseudo-nitzschia delicatissima*

Julia Boutorh, Brivaëla Moriceau, Morgane Gallinari, Olivier Ragueneau, Eva Bucciarelli

► To cite this version:

Julia Boutorh, Brivaëla Moriceau, Morgane Gallinari, Olivier Ragueneau, Eva Bucciarelli. Effect of trace metal-limited growth on the postmortem dissolution of the marine diatom *Pseudo-nitzschia delicatissima*. *Global Biogeochemical Cycles*, 2016, 30 (1), pp.57-69. 10.1002/2015GB005088. hal-01483260

HAL Id: hal-01483260

<https://hal.science/hal-01483260>

Submitted on 28 Dec 2021

HAL is a multi-disciplinary open access archive for the deposit and dissemination of scientific research documents, whether they are published or not. The documents may come from teaching and research institutions in France or abroad, or from public or private research centers.

L'archive ouverte pluridisciplinaire **HAL**, est destinée au dépôt et à la diffusion de documents scientifiques de niveau recherche, publiés ou non, émanant des établissements d'enseignement et de recherche français ou étrangers, des laboratoires publics ou privés.

Copyright



RESEARCH ARTICLE

10.1002/2015GB005088

Key Points:

- Fe and Cu limitations decrease bSiO₂ dissolution in frustules of *P. delicatissima*
- Fe- and Cu-limited *P. delicatissima* may export more Si relative to N

Supporting Information:

- Data Set S1
- Caption for Data Set S1

Correspondence to:

J. Boutorh,
julia.boutorh@univ-brest.fr;
julia.boutorh@gmail.com

Citation:

Boutorh, J., B. Moriceau, M. Gallinari, O. Ragueneau, and E. Bucciarelli (2016), Effect of trace metal-limited growth on the postmortem dissolution of the marine diatom *Pseudo-nitzschia delicatissima*, *Global Biogeochem. Cycles*, 30, 57–69, doi:10.1002/2015GB005088.

Received 6 JAN 2015

Accepted 18 DEC 2015

Accepted article online 22 DEC 2015

Published online 23 JAN 2016

Corrected 29 FEB 2016

This article was corrected on 29 FEB 2016. See the end of the full text for details.

Effect of trace metal-limited growth on the postmortem dissolution of the marine diatom *Pseudo-nitzschia delicatissima*

Julia Boutorh¹, Brivaëla Moriceau¹, Morgane Gallinari¹, Olivier Ragueneau¹, and Eva Bucciarelli¹

¹Université de Brest, CNRS, IRD, IFREMER, UMR 6539 LEMAR, OSU-IUEM, Plouzané, France

Abstract We investigated the effects of iron (Fe) and copper (Cu) limitations on biogenic silica (bSiO₂) dissolution kinetics of the marine diatom *Pseudo-nitzschia delicatissima* during a 3 week batch dissolution experiment. The dissolution of this species was faster during the first week than thereafter. Modeling results from four dissolution models and scanning electron microscopy images suggested the successive dissolution of two phases of bSiO₂, with two different dissolution constants. Micronutrient limitation during growth affected the respective proportion of the two phases and their dissolution constants. After 3 weeks of dissolution, frustules from micronutrient-limited diatoms were better preserved than those of replete cells. Our results also confirm that micronutrient-limited cells may export more Si relative to N than replete cells and may increase the silicate pump: This may not only be due to a higher degree of silicification of the live cells but also to a decoupling between the recycling of Si and N during dissolution. We suggest that a mechanistic understanding of the evolution of the dissolution constant during dissolution is needed. This would improve the parameterization of dissolution in ecosystem models, and ultimately their predictions on the amount of bSiO₂ that dissolves in the photic zone, and the amount of bSiO₂ that is exported to the seafloor.

1. Introduction

Silicon (Si) partly controls the growth of one of the major phytoplankton groups, diatoms. Indeed, diatoms use silicic acid (dSi) to grow a siliceous shell called frustule and account for 35% of the primary production in oligotrophic ocean waters and up to 75% in the Southern Ocean [Nelson *et al.*, 1995; Tréguer *et al.*, 1995]. The competition between biogenic silica (bSiO₂) recycling and export in the whole water column controls dSi availability in surface waters [Ragueneau *et al.*, 2000; Loucaides *et al.*, 2011]. Only a few field studies have been devoted to the measurement of bSiO₂ dissolution in surface waters using isotopic tracer methods [e.g., Nelson and Goering, 1977; Closset *et al.*, 2014]. The fate of bSiO₂ in the mesopelagic zone, i.e., beneath the photic zone down to 1000 m depth [Buesseler and Boyd, 2009], is also poorly studied. Hence, as stated by Van Cappellen *et al.* [2002], there is a need to identify the environmental variables that affect the dissolution process, to include mechanistic equations correctly describing dissolution rates in models of the marine silicon cycle.

Frustule bSiO₂ dissolution of free diatom cells is mainly a chemical process depending on the physico-chemical characteristics of the surrounding seawater. Numerous laboratory experiments have already been conducted investigating the effects of temperature [Kamatani, 1982], the incorporation of aluminum within the frustule [Gehlen *et al.*, 2002], the dSi concentration of seawater [Rickert *et al.*, 2002], and the specific surface area of the frustule [Dixit *et al.*, 2001] on bSiO₂ dissolution. An increasing amount of studies also indicate that the dissolution of diatom frustules might not be well represented by the commonly used exponential model [e.g., Truesdale *et al.*, 2005a; Moriceau *et al.*, 2009]. This simple, one-step dissolution process model generally constrains bSiO₂ dissolution in ocean biogeochemical models [e.g., Gehlen *et al.*, 2006; Mongin *et al.*, 2006]. It implies that all the molecules of bSiO₂ within the frustule are available for the reaction at any time, which is kinetically incorrect [Truesdale *et al.*, 2005a]. The dissolution of the frustule might rather be a multistep process, either because the frustule may be constituted of different biomineral phases with different dissolution behaviors [Gallinari *et al.*, 2002; Moriceau *et al.*, 2009] or because the specific surface area of the frustules may change during dissolution [Hurd and Birdwhistell, 1983; Truesdale *et al.*, 2005a]. Some studies have also considered the importance of biological processes on bSiO₂ dissolution, such as the existence of an organic coating surrounding the diatoms, which needs to be removed by bacteria prior to dissolution [Bidle and Azam, 2001], or the effect of grazing on diatom dissolution [Schultes *et al.*, 2010].

Also, environmental growth conditions, like nutrient availability, influence the degree of silicification of the frustule [Claquin *et al.*, 2002] as well as the cell stoichiometry [Geider and La Roche, 2002]. However, to our knowledge, no study has directly measured the effect of changes in silicification induced by nutrient limitation on diatom bSiO₂ dissolution.

Amongst nutrients essential to life are trace metals: Their abundance and cycling in the oceans change the abundance and biodiversity of marine biota [de Baar and La Roche, 2003]. During the last two decades, it has been convincingly shown that the subnanomolar oceanic concentrations of iron (Fe) are low enough to limit primary production in ~50% of the world's oceans, including the Southern Ocean where diatoms dominate the phytoplanktonic community [Boyd and Ellwood, 2010]. Fe limitation also induces a decoupling in the use of major macronutrients by phytoplankton, which is likely to influence the cycling of the major biogeochemical cycles (C, N, P, and Si) over geological time scales [de Baar and La Roche, 2003]. Fe-limited diatoms generally increase their consumption of silicate relative to nitrate, which increases their Si:N and Si:C ratios [Marchetti and Cassar, 2009, and references therein]. It is generally assumed, according to Boyle's hypothesis, that more silicified, Fe-limited diatoms would sink faster than replete cells and would export more Si than C and N to the bottom of the ocean [Boyle, 1998]. A recent study highlights that hot spots of Si burial in the Southern Ocean, the North Pacific, and in continental margins are characterized by high Si: organic carbon export ratios, resulting from Fe limitation of diatoms during growth [Pichevin *et al.*, 2014]. Another trace metal, copper (Cu), may also limit phytoplankton growth in the open ocean [Coale, 1991; Peers *et al.*, 2005]. It has also been hypothesized that due to physiological interactions, Cu limitation may be linked to Fe limitation [Peers *et al.*, 2005; Maldonado *et al.*, 2006; Peers and Price, 2006]. If Cu limitation indeed essentially results in Fe limitation [Maldonado *et al.*, 2006], then Cu limitation could induce a decoupling between Si, N, and C. Such decoupling has important consequences on particle export and the cycling of the major nutrients. Determining whether Fe or Cu limitation during diatom growth affects postmortem frustule dissolution would lead to a better understanding of the processes affecting bSiO₂ dissolution in the water column and would ultimately improve our knowledge of Si cycling.

In the present study, we focused on the effects of micronutrient-limiting conditions during growth on the post-mortem dissolution of frustules from nutrient replete, Cu-limited, and Fe-limited cells of *Pseudo-nitzschia delicatissima* by performing a 22 day dissolution experiment. *P. delicatissima* is an ubiquitous species that can dominate Fe-limited open ocean waters [Gómez *et al.*, 2007]. Besides, *Pseudo-nitzschia* is a genus that often dominates artificially [Trick *et al.*, 2010] and naturally [Queguiner, 2013, and references therein] Fe-fertilized blooms. Kinetic constants of bSiO₂ dissolution of these frustules were estimated by running four different models. By following changes in the Si:N elemental ratios of diatoms during their dissolution, we also revisit Boyle's hypothesis [1998].

2. Materials and Methods

2.1. Culture Conditions

Pseudo-nitzschia delicatissima is a small (approximately 100 μm³), solitary diatom species, which was isolated in 2008 in the Bay of Brest, France (strain Pd08RB) by Beatriz Beker. Batch cultures were grown in duplicate in 10 L polycarbonate carboys at 18°C under fluorescent light (Vita Lite Plus, Durotest) at a light intensity of 212 μmol photons m⁻² s⁻¹ and a 12:12 light:dark cycle. Previous, extensive culture work was conducted on that clone in our laboratory to investigate how Fe and Cu (co) limitations affect its physiology [Lelong *et al.*, 2013; Le Grand *et al.*, 2015]. It provided us a robust working basis to determine the level of Cu and Fe where growth limitation could be achieved and to assess that our duplicate cultures grew as previous triplicate or quadruplicate cultures did.

Sterile, trace metal clean techniques were applied at all times during the culture work [Sunda *et al.*, 2005]. The complete media consisted of artificial Aquil sea water as described in Price *et al.* [1988–1989], enriched with macronutrients (300 μmol L⁻¹ nitrate, 10 μmol L⁻¹ phosphate, and 100 μmol L⁻¹ silicate), vitamins (0.55 μg L⁻¹ vitamin B12, 0.5 μg L⁻¹ biotin, and 100 μg L⁻¹ thiamin), and trace metals (10 nmol L⁻¹ of Se, 100 nmol L⁻¹ of Mo, 50.3 nmol L⁻¹ of Co, 79.7 nmol L⁻¹ of Zn, 121 nmol L⁻¹ of Mn, 500 nmol L⁻¹ of Fe, and 19.6 nmol L⁻¹ of Cu). Ethylenediaminetetra acetic acid (100 μmol L⁻¹) buffered the media for trace metals. It generated free ion concentrations of Fe, Cu, Co, Zn, and Mn of 10^{-19.2}, 10^{-13.9}, 10⁻¹¹, 10^{-10.7}, and 10^{-8.14} mol L⁻¹, respectively, for nonilluminated media at pH 8.1 and 18°C according to the chemical equilibrium program MINEQL+ (version 4.62.3). In the Fe-limited medium, 5 nmol L⁻¹ of Fe ([Fe³⁺] = 10^{-21.2} mol L⁻¹) was added instead of 500 nmol L⁻¹.

Table 1. Specific Growth Rates, Biogenic Silica Quotas, Cell Dimensions, Surface Areas, and Si:N Molar Ratios of the Replete, Copper-Limited, and Iron-Limited Cells of *P. delicatissima* During Growth^a

	Replete	Cu Limitation	Fe Limitation
Specific growth rate (d ⁻¹)	1.24 ± 0.05 (n = 2)	0.73 ± 0.02 (n = 2)	0.32 ± 0.01 (n = 2)
Biogenic silica (pmol cell ⁻¹)	0.12 ± 0.01 (n = 3)	0.13 ± 0.01 (n = 4)	0.06 ± 0.02 (n = 4)
Apical length (μm)	17.9 ± 0.4 (n = 50)	20.0 ± 0.5 (n = 51)	20.1 ± 0.3 (n = 100)
Transapical width (μm)	3.4 ± 0.1 (n = 50)	3.3 ± 0.1 (n = 51)	2.4 ± 0.1 (n = 100)
Surface area (μm ²)	152 ± 6 (n = 50)	164 ± 8 (n = 51)	119 ± 7 (n = 50)
Biogenic silica (fmol μm ⁻²)	0.81 ± 0.07 (n = 3)	0.76 ± 0.03 (n = 4)	0.52 ± 0.14 (n = 4)
Si:N (mol mol ⁻¹)	0.63 ± 0.08 (n = 3)	0.50 ± 0.04 (n = 4)	1.21 ± 0.37 (n = 4)

^aResults are presented as the means ± 95% confidence interval (CI). Values in brackets are the number of measurements used to calculate the average and CI.

There was no copper addition for the Cu-limited condition. Cell concentrations were measured with a flow cytometer FACSCalibur (BD Sciences) with an argon blue laser (488 nm). Specific growth rate (μ) was determined by linear regression of the natural logarithm of the cell concentration versus time.

Diatoms were preacclimated to Fe limitation, Cu limitation, and replete conditions until their growth rate remained stable over several days. The cells were then grown at a constant growth rate for at least 10 generations before samplings. Total biomass was maintained low enough during growth so that pH remained below 8.5 and CO₂ limitation was avoided (~50,000–200,000 cells mL⁻¹, i.e., ~3–13 μL_{cell} L⁻¹ as calculated by multiplying the average cell volume by the number of cells per liter of culture medium). Fe limitation and Cu limitation decreased the specific growth rate of the cells by 75% and 40%, respectively, compared to nutrient-replete cells (Table 1). This is similar to the decreases that were measured at the same trace metal concentrations (65% at 5 nM of total Fe and 34% at 0 nM of total Cu [Lelong et al., 2013], and 34% at 0 nM of total Cu in quadruplicate cultures [Le Grand et al., 2015]). Prior to filtering the cultures for conducting the dissolution experiments, samples were collected in triplicate in each carboy for analysis of cell concentrations, particulate organic nitrogen (PON), and biogenic silica (bSiO₂) (Table 1). For each culture condition the average cell volume and surface area were calculated as an ellipsoid from measurements of the transapical width (a , μm) and apical length (A , μm) of more than 50 randomly selected cells using software image analysis (Visilog 5) after digitization with an analogic Leica camera [Leynaert et al., 2004]:

$$\begin{aligned} \text{Volume} &= (\pi_* a^2 A) / 6 \\ \text{Surface} &= 0.5_* \pi_* a^2 + [\pi_* a_* A_* \arcsin(e)] / (2_* e) \\ \text{with eccentricity } e &= (1 - a^2/A^2)^{1/2} \end{aligned}$$

The remaining cultures for each treatment (i.e., two carboys) were pooled and filtered onto 1 μm polycarbonate filters, resuspended in ~30 mL of artificial sea water, and frozen at –20°C for at least a month before the dissolution experiment was conducted. Flow cytometry analyses showed that freezing at –20°C did not change the cell size (as estimated by forward scatter measurements) nor the cell complexity (as estimated by side scatter measurements).

2.2. Dissolution Experiments

After slowly thawing at room temperature, frozen cells were resuspended in natural filtered seawater in a 10 L polycarbonate bottle for each growth condition (i.e., replete, Cu limitation, and Fe limitation). This seawater, collected in the Bay of Brest, was filtered using 0.7 μm Whatman GF/F filters to preserve most of the natural bacterial community and to remove phytoplankton and grazers. Silicic acid (dSi) concentration in the filtered seawater was below 5 μmol L⁻¹, which allows the dissolution to take place (saturation level at 20°C is close to 1300 μmol L⁻¹) [Dixit et al., 2001]. Concentrations of dead diatoms were 160,000 cells mL⁻¹ (Fe-limited treatment), 200,000 cells mL⁻¹ (Cu-limited treatment), and 250,000 cells mL⁻¹ (replete treatment) on the first day of the experiment (T_0). Dead diatoms were incubated for 22 days, and each experiment was conducted in the dark at 17°C. We also measured the bacterial concentrations in the different carboys at the beginning of the dissolution experiment by flow cytometry [Lelong et al., 2011]. The initial bacteria concentrations were 1.6 × 10⁶ bacteria mL⁻¹ in the replete treatment, 2.6 × 10⁶ bacteria mL⁻¹ in the Cu-limited treatment, and 3.0 × 10⁶ bacteria mL⁻¹ in the Fe-limited treatment. These concentrations are sufficient to remove the organic coating within 4 days and start the dissolution

process [Bidle and Azam, 1999]. Incubated carboys were homogenized with a magnetic stirrer to limit the formation of aggregates. Every day during the first week and three times per week afterward, each carboy was homogenized by 50 reversals and subsampled in three 125 mL polycarbonate bottles. Samples for bSiO₂, dSi, and PON were then collected from each bottle and analyzed as described below. Technical replicates were regularly analyzed during the experiment (see supporting information). Oxygen saturation levels and pH were measured daily. During the course of the experiments, oxygen saturation levels varied between 74% and 100%, which ensured that the conditions were not hypoxic, while pH varied between 7.1 and 8.1.

2.2.1. Analytical Methods

2.2.2. bSiO₂

Samples were filtered on 0.6 μm polycarbonate filters, rinsed with artificial seawater, and dried at 60°C overnight. Filters were digested in 20 mL NaOH (0.2 mol L⁻¹) for 3 h at 95°C and stirred regularly to ensure complete dissolution of bSiO₂. Solutions were neutralized with 5 mL HCl (1 mol L⁻¹), centrifuged, and supernatants were analyzed for dSi [Ragueneau and Tréguer, 1994; Moriceau et al., 2007].

2.2.3. dSi

Silicic acid concentrations were measured in 0.6 μm filtered seawater samples and in the digested bSiO₂ samples using the molybdate blue spectrophotometric method of Mullin and Riley [1965], as adapted by Tréguer and Le Corre [1975] and modified by Gordon et al. [1993] for use in segmented flow colorimetry with a Luebbe Technicon Autoanalyzer (precision, as relative standard deviation RSD, <1%).

2.2.4. PON

Samples were filtered on precombusted Whatman GF/F filters (450°C for 4 h) and rinsed with artificial seawater containing no nutrients. The filters were dried at 60°C overnight in precombusted glassware and stored until analysis using a Thermo Fisher NA 2100 CN elemental analyzer (precision, as RSD, 1%).

2.3. Modeling Experiment

To understand the processes that control bSiO₂ dissolution of *P. delicatissima*, to calculate the kinetic parameters of these processes, and finally to compare the effects of Fe and Cu limitation on the postmortem dissolution of *P. delicatissima*, four mechanistic models were run. For each dissolution experiment, the models reconstructed the temporal evolution of dSi and bSiO₂ concentrations, both of which were independently measured parameters in our experiments. The successive models were based on equations of increasing complexity. Results from the four models were compared statistically.

2.3.1. Models

The first model is the most commonly used and assumes a one-step dissolution process (equation (1)), using a simple first-order rate equation [Greenwood et al., 2001]:

$$\hat{C}_{(t)} = C_0 \cdot e^{-k \cdot t} \quad (1)$$

where $\hat{C}_{(t)}$ is the modeled bSiO₂ concentration (μmol L⁻¹) calculated at time t (day), C_0 is the initial bSiO₂ concentration (μmol L⁻¹) at T_0 , and k is the dissolution constant (d⁻¹).

The second model assumes the evolution of the specific surface area of two different physical fractions of the frustules (e.g., fractions with different shapes or morphologies) [Loucaides et al., 2011; Truesdale et al., 2005b] or the simultaneous dissolution of two different chemical phases of biogenic silica (e.g., different degrees of hydration or presence of impurities) [Loucaides et al., 2011; Moriceau et al., 2009]:

$$\hat{C}_{(t)} = C_1 \cdot e^{-k_1 \cdot t} + C_2 \cdot e^{-k_2 \cdot t} \quad (2)$$

C_1 and C_2 are the concentrations (μmol L⁻¹) of two different physical fractions [Truesdale et al., 2005a] or chemical phases [Moriceau et al., 2009], and k_1 and k_2 (d⁻¹) are their respective dissolution constants.

A better fit to the data using the third model (equations (3a) and (3b)) could be interpreted as two different phases of biogenic silica dissolving one after the other (e.g., one protecting the other), or as a change in the dissolution constant during dissolution, due to changes in environmental conditions (e.g., pH, temperature, and bacterial activity) [Moriceau et al., 2009].

$$\hat{C}_{(t)} = C_0 \cdot e^{-k_1 \cdot t}; 0 < t < t_s \quad (3a)$$

$$\hat{C}_{(t)} = C_{t_s} \cdot e^{-k_2 \cdot (t - t_s)}; t > t_s \quad (3b)$$

Like model 2, it calculates four parameters. C_0 is the initial bSiO₂ concentration ($\mu\text{mol L}^{-1}$) at T_0 . At substitution time t_s (day), the dissolution constant changes from k_1 to k_2 (d^{-1}), with C_{t_s} the concentration of bSiO₂ ($\mu\text{mol L}^{-1}$) at t_s .

The fourth model describes the dissolution of two physical fractions with different specific surface area, or the dissolution of two different chemical bSiO₂ phases, one partially protecting the other:

$$\hat{C}(t) = C_1 \cdot e^{-k_1 \cdot t} + C_2 \quad (4a)$$

$$\hat{C}(t) = C_1 \cdot e^{-k_1 \cdot t} + C_2 \cdot e^{-k_2 \cdot (t - t_s)} \quad (4b)$$

Model 4 calculates five parameters. During the first dissolution step and before substitution time t_s (day), only the first fraction, or phase of bSiO₂, at concentration C_1 ($\mu\text{mol L}^{-1}$), dissolves with dissolution constant k_1 (d^{-1}). After t_s a second fraction, or phase, at concentration C_2 ($\mu\text{mol L}^{-1}$) starts to dissolve simultaneously with dissolution constant k_2 (d^{-1}).

2.3.2. Statistical Analyses

Statistical analyses were performed to evaluate the goodness of fit of each model (i.e., how well experimental data were described by each model) and the robustness of the calculated parameters and to compare the validity of the different models.

The goodness of fit of the different models was compared by calculating a log-likelihood statistics (Log(L), equation (5)) [Hilborn and Mangel, 1997].

$$\log(L) = -\frac{N}{2} * \left[\log \left[\left(\frac{\sum (\hat{C}_j - C_j)^2}{N} \right) + 1 \right] \right] \quad (5)$$

Log(L) calculates the difference between a modeled value and the experimental value, taking into account all data. N is the total number of data. At " j " time, C_j is the measured concentration and \hat{C}_j is the modeled concentration.

For the same complexity, i.e., for the same number of modeled parameters, the higher Log(L), the better the goodness of fit. However, Log(L) of models of increasing complexity (i.e., increasing degrees of freedom) will mathematically be better. To properly compare the goodness of fit between these models, Log(L) of the best model should be at least 2 units higher per added parameter than Log(L) of the other models [Hilborn and Mangel, 1997]. For example, model 3 uses two more parameters than model 1 to calculate the bSiO₂ concentrations. Model 3 would better fit the experimental data than model 1 only if Log(L) of model 3 is at least 4 units higher than Log(L) of model 1.

The standard deviation (root-mean-square deviation, RMSD) and the coefficient of variation of RMSD (CV_{RMSD}) of the calculated kinetics parameters were calculated using the Jackknife method.

3. Results

Although carboys were stirred and mixed by 50 reversals before samplings, we could see that aggregates formed from the fifth to the tenth day in the replete and Cu-limited carboys. Total Si (i.e., bSiO₂ + dSi, Figure 1) concentrations also significantly decreased in the replete and Cu-limited carboys from $32.9 \pm 1.4 \mu\text{mol L}^{-1}$ ($n=24$, CI=95%) and $38.6 \pm 2.5 \mu\text{mol L}^{-1}$ ($n=25$, CI=95%), respectively, in nonaggregate conditions, to $25.8 \pm 1.3 \mu\text{mol L}^{-1}$ ($n=6$, CI=95%) and $29.2 \pm 1.3 \mu\text{mol L}^{-1}$ ($n=6$, CI=95%), respectively, during aggregation. It suggests a bias in particulate, i.e., bSiO₂, sampling.

We did not see aggregates in the Fe-limited carboy likely due to the approximately tenfold lower concentration of chlorophyll in that treatment compared to the others. However, total Si concentrations also decreased in that carboy from $17.6 \pm 0.7 \mu\text{mol L}^{-1}$ ($n=7$, CI=95%) for the first 7 days to $15.4 \pm 0.6 \mu\text{mol L}^{-1}$ ($n=13$, CI=95%), during the last 15 days. It strongly suggests aggregation from day 8. Due to a possible bias in particulate sampling during aggregation, concentrations of bSiO₂ and PON were not validated during these times. However, the elemental ratio of the particles should not change whether they are homogeneously sampled or not. As a result, Si:N ratio was calculated during the whole experiment. Besides, aggregates should not have affected the dissolution rates calculated in our experiments. The decrease of bSiO₂ dissolution

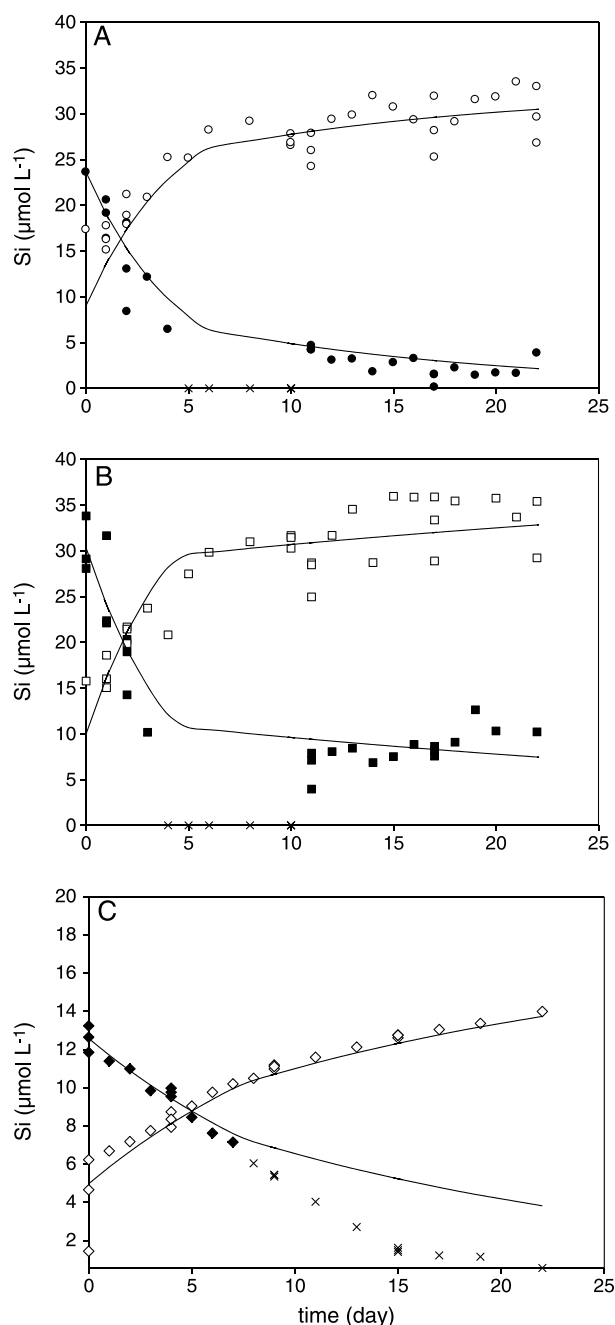


Figure 1. Temporal evolution of bSiO₂ concentrations (µmol L⁻¹, filled symbols) and dSi concentrations (µmol L⁻¹, open symbols) in the three treatments: (a) frustules of replete cells, (b) frustules of Cu-limited cells, and (c) frustules of Fe-limited cells. Black lines represent fitting of the data by model 3. Due to aggregate formation, some bSiO₂ data have not been considered for the modeling experiment (black crosses), as explained in section 3.

(0.99–1.00) and decreased to 0.97 at the end of the dissolution. Consequently, bSiO₂ dissolution rates were not affected by dSi concentration in seawater in the three carboys during the dissolution experiment.

3.2. Biogenic Silica Concentrations

Concentrations of bSiO₂ were measured in the three carboys throughout the dissolution experiment (Figures 1a–1c). The bSiO₂ concentration for the Cu-limited treatment at T₀ (30.3 ± 3.5 µmol L⁻¹, n = 3, CI = 95%)

rates in aggregates is known to occur when cells are still alive within the aggregates [Moriceau et al., 2007; Passow et al., 2011] or when the degradation rate of organic coating decreases over time [Passow et al., 2011]. Cells were dead in our dissolution experiments, and aggregates formed after day 4, when most of the organic coating had already been degraded by bacteria [Bidle and Azam, 1999]. Moreover, we did not observe any change in the dissolution kinetics when aggregates disappeared. Finally, the exchangeable pore water content occupies 87–98% of the aggregate volume [Ploug and Passow, 2007], which is enough not to affect the surface area exposed to dissolution.

3.1. Silicic Acid Concentrations

Concentrations of dSi were measured in the three carboys throughout the dissolution experiment (Figures 1a–1c). Initial dSi concentrations were higher for the replete and Cu-limited treatments (17.3 µmol L⁻¹ and 15.8 µmol L⁻¹, respectively) than for the Fe-limited treatment (4.1 ± 2.8 µmol L⁻¹, n = 3, CI = 95%). During the dissolution experiment, dSi concentrations increased up to 33.5 µmol L⁻¹ for the replete treatment, 36.0 µmol L⁻¹ for the Cu-limited treatment, and 14.0 µmol L⁻¹ for the Fe-limited treatment. Because bSiO₂ dissolution rates depend on the degree of undersaturation σ (equation (6)), we calculated σ in our experimental conditions to evaluate the possible differences between the carboys.

$$R = k * \sigma \quad (6)$$

[Rickert et al., 2002, and references therein]

where R is the dissolution rate, k is the dissolution constant, and σ is the degree of undersaturation, defined as

$$\sigma = 1 - C/C_{eq} \quad (7)$$

[Van Cappellen, 1996] with C the dSi concentration in seawater and C_{eq} the equilibrium solubility of bSiO₂.

In our experiments, σ was similar in all treatments at the beginning of the dissolution

Table 2. Log-Likelihood Statistics (Log(L)) Calculated for the Four Models for bSiO₂ Dissolution of Frustules of Replete, Fe-Limited, and Cu-Limited Cells^a

	Replete	Cu-Limited	Fe-Limited
Log (<i>L</i> _{M1})	90.6	80.8	99.8
Log (<i>L</i> _{M2})	95.8	96.9	108.0
Log (<i>L</i> _{M3})	96.8	96.9	109.1
Log (<i>L</i> _{M4})	96.3	96.8	109.6

^aValues in italics indicate the models which give the best goodness of fit according to the log-likelihood statistics.

was higher than for the replete treatment (23.6 μmol L⁻¹). At *T*₀ the bSiO₂ concentration of the Fe-limited treatment (12.6 ± 0.8 μmol L⁻¹, *n* = 3, CI = 95%) was ~2 times lower than for the replete treatment.

bSiO₂ dissolution rates depend on initial bSiO₂ concentrations (equations (1)–(3a), (3b), (4a), (4b)). To properly compare the biogenic silica dis-

solution kinetics between the different treatments, all bSiO₂ concentrations were normalized to the initial concentrations.

3.3. Biogenic Silica Dissolution Kinetics of *P. delicatissima*

During aggregate formation, only dSi concentration data were used for the modeling experiment. Both dSi and bSiO₂ concentrations data were used otherwise to run the models.

For all three treatments, model 4 was disregarded, as Log(*L*_{M4}) was never two points higher than Log(*L*_{M2}) or Log(*L*_{M3}) (Table 2). For the replete and Fe-limited treatments, model 3 better fits the data compared to models 1 and 2 (Table 2). For the Cu-limited treatment, models 2 and 3 better described the dissolution process than model 1, and Log(*L*_{M2}) and Log(*L*_{M3}) were similar. The dissolution constant *k*₂, however, was calculated with a better precision by model 3 (14%) than by model 2 (67%), while *k*₁ was equally precise with both models (3–4%). Therefore, model 3 best reconstructed bSiO₂ dissolution in all treatments than the other models.

In all three treatments, the substitution times (*t*_s) were close to each other (from 4.5 to 7.5 days) and frustules dissolved faster before *t*_s than after *t*_s (Table 3). bSiO₂ dissolution kinetics of frustules of the replete and Cu-limited cells were similar before *t*_s, as assessed by the same value of *k*₁. After *t*_s, however, frustules of replete cells dissolved 3.5 times faster than frustules of Cu-limited cells (Figure 1 and Table 3). Frustules of Fe-limited cells dissolved ~3 times slower than the frustules of the other treatments before *t*_s. After *t*_s they still dissolved ~1.5 times slower than frustules of replete cells, but ~2 times faster than frustules of Cu-limited cells (Table 3). Before *t*_s, frustules of Fe-limited cells were better preserved (59% of bSiO₂ remained) than those of Cu-limited and replete cells (37% and 24% of bSiO₂ remained, respectively) (Table 3). After 22 days of dissolution, ~30% of the initial bSiO₂ remained at the end of the experiment in the Cu-limited and Fe-limited treatments, while ~9% only remained in the replete treatment.

Dissolution kinetics for the three treatments were consistent with other studies that describe a two-step dissolution of the frustules [Kamatani, 1982; Roubex et al., 2008], with *k*₁ values higher than *k*₂ values. Dissolution constants from our modeling experiment were in the range of dissolution constants reported in other laboratory studies on bacteria-mediated dissolution of fresh or cleaned diatom frustules (0.004 to 0.41 d⁻¹) [Roubex et al., 2008, and references therein]. Our *k*₁ for frustules of replete and Cu-limited cells was close to the highest values from the literature: 0.18 d⁻¹, 0.27 d⁻¹, and 0.41 d⁻¹ for the dissolution of

Table 3. Dissolution Constants Calculated by Model 3 for Frustules of Replete, Fe-Limited, and Cu-Limited Cells ± the Root-Mean-Square Deviation (RMSD)^a

	<i>C</i> ₀ (μM)	CV _{RMSD}	% Phase 1	<i>k</i> ₁ (d ⁻¹)	CV _{RMSD}
Replete cells	1.07 ± 0.02	0.02	76	0.22 ± 0.01	0.04
Cu-limited cells	1.09 ± 0.01	0.01	63	0.23 ± 0.01	0.04
Fe-limited cells	0.97 ± 0.004	0.004	41	0.072 ± 0.001	0.01
	<i>t</i> _s (d)	CV _{RMSD}	% Phase 2	<i>k</i> ₂ (d ⁻¹)	CV _{RMSD}
Replete cells	5.9 ± 0.2	0.04	24	0.068 ± 0.003	0.05
Cu-limited cells	4.5 ± 0.3	0.06	37	0.021 ± 0.003	0.13
Fe-limited cells	7.5 ± 0.3	0.04	59	0.045 ± 0.001	0.03

^aCV_{RMSD} is the coefficient of variation calculated from the Jackknif method. The respective proportion of the two phases of bSiO₂ that constitute the frustule is calculated (% phase 1 and % phase 2), as well as their respective dissolution constants *k*₁ and *k*₂ (d⁻¹).

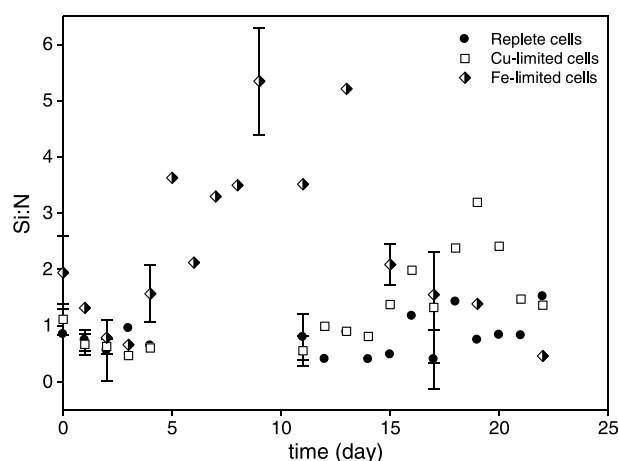


Figure 2. Temporal evolution of Si:N molar ratios of frustules from the three treatments. The error bars represent the standard deviation (SD), calculated from triplicate samplings of bSiO_2 and PON during the remineralization experiments. Between day 5 and day 10, bSiO_2 values were below the detection limit of our analytical method ($0.5 \mu\text{mol L}^{-1}$), which prevented to calculate Si:N in the replete and Cu-limited treatments.

the dissolution experiment (Figure 2). Elemental ratios were more precise at T_1 than at T_0 , probably due to a better homogenization at T_1 (1.31 , 0.67 ± 0.19 , and $0.74 \pm 0.19 \text{ mol mol}^{-1}$, for frustules of Fe-limited, Cu-limited, and replete cells, respectively), and comparable to the elemental ratios measured during cell growth in the three different Aquil media (Table 1). This is the first time to our knowledge that the Si:N ratio of a Cu-limited diatom is measured during growth. It indicates that contrary to Fe limitation, Cu limitation does not increase Si:N in live diatoms, compared to replete cells (Table 1). This is consistent with previous conclusions from *Lelong et al.* [2013], indicating that at the physiological level, *P. delicatissima* does not display the same changes under Cu limitation and Fe limitation. Besides, during dissolution, Si and N were not recycled at the same rate in the micronutrient-limited treatments and in the replete treatment. As a result, different Si:N ratios were measured during dissolution in the three treatments.

The Si:N ratio in the replete treatment was constant throughout the experiment (Figure 2, $0.80 \pm 0.16 \text{ mol mol}^{-1}$, $n=17$, $\text{CI}=95\%$). In the Cu-limited treatment, Si:N was also constant during the first 14 days ($0.75 \pm 0.14 \text{ mol mol}^{-1}$, $n=9$, $\text{CI}=95\%$). From day 15 until the end of the experiment, however, Si:N of Cu-limited cells significantly increased to $1.94 \pm 0.47 \text{ mol mol}^{-1}$ ($n=8$, $\text{CI}=95\%$). In the Fe-limited treatment, Si:N increased sharply from $1.25 \pm 0.50 \text{ mol mol}^{-1}$ before day 5 ($n=5$, $\text{CI}=95\%$) to $3.80 \pm 0.84 \text{ mol mol}^{-1}$ ($n=7$, $\text{CI}=95\%$) between days 5 and 13. Over the last several days of the experiment, the Si:N ratio returned to a value similar to that measured at the beginning of the experiment (Figure 2).

The Si:N of frustules of replete cells were lower than Si:N of frustules of Cu-limited cells during the last week of dissolution (approximately twofold difference). They were also lower than those of Fe-limited cells at all times (1.4 to 5.9-fold difference), except for the third (1.4 times higher) and last day (3.3 times higher).

4. Discussion

4.1. Impact of Fe and Cu Limitations on the Dissolution of *P. delicatissima*

Most of dissolution experiments show a two-step dissolution of diatom frustules [*Truesdale et al.*, 2005b, and references therein]. Our modeling experiments confirmed this trend: Frustules of *P. delicatissima* dissolved faster during the first 6 days of the experiment than thereafter (Table 3). The same model best fitted the dissolution of the frustule of *P. delicatissima* in all three treatments, i.e., whatever the growth conditions of the living cells. Equations of model 3 may describe the dissolution of two phases of bSiO_2 , or changes in the dissolution constant during dissolution, due to changes in environmental conditions, e.g., pH, temperature, or bacterial activity [*Gallinari et al.*, 2002; *Moriceau et al.*, 2009]. In our case, physico-chemical properties of seawater (pH, temperature, pressure, and salinity) were constant during the dissolution experiment and

acid-cleaned frustules of *Eucampia zodiacus* [*Kamatani*, 1982], of fresh *Skeletonema marinoi* [*Moriceau et al.*, 2009], and of cleaned frustules of *Rhizosolenia hebetate* [*Kamatani and Riley*, 1979], respectively.

3.4. Particulate Organic Nitrogen Concentrations

The PON concentration at T_0 was lower for the Fe-limited treatment ($6.5 \pm 2.0 \mu\text{mol L}^{-1}$, $n=3$, $\text{CI}=95\%$) than for the replete treatment ($28.0 \pm 14.8 \mu\text{mol L}^{-1}$, $n=2$, $\text{CI}=95\%$) and the Cu-limited treatment ($27.3 \pm 5.8 \mu\text{mol L}^{-1}$, $n=2$, $\text{CI}=95\%$). Normalized to the PON concentration at T_0 , $\sim 9\%$ and $\sim 28\%$ of residual PON remained at the end of the experiment for the replete and the Cu-limited treatments, respectively.

3.5. Evolution of the Si:N Molar Ratios

The evolution of Si:N molar ratio was calculated for the three treatments throughout

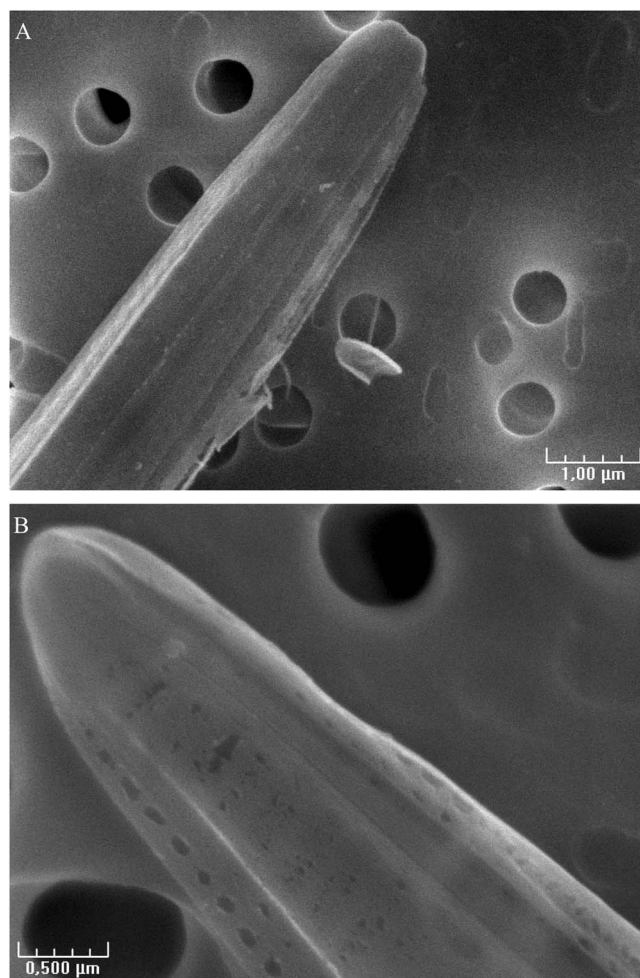


Figure 3. Scanning electron microscopy (SEM) images of frustules from Fe-limited cells after (a) 5 days of dissolution and (b) 30 days of dissolution.

Scanning electron microscopy (SEM) images were taken during the dissolution of frustules of Fe-limited cells (Figures 3a and 3b). These pictures tend to show that the frustules were getting more porous as dissolution proceeded, which suggests an increase in SSA. Similarly, *Hurd and Takahashi* [1983] and *Frayse et al.* [2009] report that the SSA of radiolarian skeletons and phytoliths, respectively, increases with time during dissolution. This should increase the dissolution rate with time [*Greenwood et al.*, 2001], which is contrary to what we observed. Previous studies to explain the evolution of the dissolution constant with time also strongly suggest the successive dissolution of two phases of bSiO_2 , with two different dissolution constants [*Gallinari et al.*, 2002; *Moriceau et al.*, 2009]. When all of these clues are considered together, they tend to support in our experiments the hypothesis of two phases of bSiO_2 , one protecting the other. These two phases may have dissolved differently because they have different chemical properties, or because they are associated to more or less refractory pools of OM, or both. This debate will not be closed, however, as long as a mechanistic understanding of the evolution of the dissolution constant will not be studied in more detail.

In any case, our results report the first experimental evidence that Fe and Cu limitations during the growth of a diatom affect the dissolution of its frustule. These growth conditions changed the proportion of the two bSiO_2 phases in the frustule of *P. delicatissima* and their dissolution constants (Table 3). The most labile phase constituted the greater part of the frustules when cells were grown under replete or Cu-limited conditions (76% and 63% of the whole bSiO_2 , respectively) but only 41% of the total bSiO_2 of Fe-limited frustules (Table 3). The dissolution rate of a frustule depends on the chemical properties of the bSiO_2 (e.g., degree of hydration and condensation, and presence of impurities) [*Loucaides et al.*, 2011]. Our results suggest that

cannot explain our observations. Changes in bacterial abundance or activity may also change the dissolution constant during dissolution. *Bidle and Azam* [1999] evidenced that bacterial degradation of the organic coating increases the dissolution rate as the surface of frustule exposed to seawater increases. In our experiments, however, k decreased over time, which would invalidate a predominant effect of bacterial activity on dissolution rate. However, another possibility involving bacterial activity may be through interactions between organic matter (OM) and bSiO_2 within the frustule. *Moriceau et al.* [2009] report that a less soluble bSiO_2 phase is associated with more refractory OM, which may protect bSiO_2 from dissolution. If the bacterial community could not grow during our experiments or could not degrade this refractory pool of OM, the dissolution of the associated bSiO_2 may indeed have been impeded.

It must also be noted that previous studies explained changes in the dissolution constant over time by the evolution of the specific surface area (SSA) of the frustule [*Loucaides et al.*, 2011, and references therein]. Observations tend to indicate that this hypothesis is unlikely to explain the decrease of the dissolution constant in our experiments.

the chemical composition of the frustule may change during growth depending on micronutrient availability and control the respective proportions of the different phases and their dissolution constants. Because of the importance of such a process on the global biogeochemical cycle of Si, this hypothesis requires further investigation.

In the end, frustules of micronutrient-limited *P. delicatissima* dissolved less than those of replete cells, with ~70% versus 91% of the initial bSiO₂ being dissolved after 3 weeks, respectively. A common assumption is that Fe-limited diatoms would dissolve more slowly than replete ones and export more Si below the euphotic zone, due to a more silicified frustule [Boyle, 1998]. If we indeed showed a slower dissolution of frustules of Fe-limited *P. delicatissima*, we also evidenced that it was not due to a higher degree of silicification: Fe-limited cells of *P. delicatissima* are less silicified than replete ones (Table 1).

4.2. Impact of Micronutrient (Fe, Cu) Limitation on Si Export

A mechanistic understanding of diatom dissolution in seawater is important to simulate the recycling and the fate of bSiO₂ within the water column. Water column bSiO₂ dissolution constants, which are generally measured in surface waters using the ³⁰Si tracer method, range from 0.027 d⁻¹ to 0.27 d⁻¹ (10 yr⁻¹ to 100 yr⁻¹) [Nelson and Brzezinski, 1997, and references therein]. Our dissolution constants are within this range, with the second dissolution constant close to the lower limit. These dissolution constants reflect an efficient recycling of silica: 10% to 100% of the bSiO₂ is produced and dissolves in the euphotic zone [Nelson et al., 1995; Tréguer et al., 1995].

Even if the majority of biogenic silica dissolution experiments indicate a two-step dissolution of bSiO₂ [Truesdale et al., 2005b, and references therein], to our knowledge, ocean biogeochemical models do not use two consecutive dissolution constants to simulate the postmortem fate of diatoms in the water column. The value of the dissolution constant used to parameterize biogenic silica dissolution generally ranges from 0.01 d⁻¹ [Gehlen et al., 2006; Mongin et al., 2006] to 0.12 d⁻¹ [Pondaven et al., 1998; Gnanadesikan, 1999]. Our dissolution constants k_1 and k_2 are both within this range. We investigated how using k_1 and k_2 successively in parameterizing biogenic silica dissolution would impact the estimation of the preservation of bSiO₂. In our study, the percentage of bSiO₂ from *P. delicatissima* at the end of the dissolution experiment is called the preservation capacity. For frustules from replete cells, the use of k_1 alone gives an underestimated preservation capacity of less than 1%, whereas the use of k_2 alone gives an overestimated preservation capacity of 21%. The preservation capacity is 9% of the initial bSiO₂ when both k_1 and k_2 are used. Therefore, taking into account a two-step dissolution process during the settling to the sea floor of the diatoms is important to estimate the amount of bSiO₂ dissolving in the photic zone, reenriching the water column in dSi, and sustaining the growth of new cells and the amount of bSiO₂ reaching the sea floor. Besides, when using the two dissolution constants, the preservation capacity of frustules of Cu-limited and Fe-limited cells increased to 25% and 29%, respectively, which is almost threefold higher than the preservation capacity of frustules of replete diatoms. Although these calculations were made by using k values from laboratory-controlled cultures of a single species of diatom and are therefore difficult to extrapolate to natural ecosystems, they support the assumption of Pichevin et al. [2014] that Si burial increases when diatoms have grown under Fe stress. If similar results were to be reported for other species of diatoms or mixed planktonic communities, they would have important consequences on the estimation of bSiO₂ preservation.

As such, we need to better understand the chemical, physical, and biological processes that control the dissolution constants over time which may ultimately lead to a better parameterization of the bSiO₂ dissolution in global ecosystems models. Moreover, to our knowledge, these are the first direct measurements giving evidence of an effect of micronutrient availability during growth on the postmortem dissolution kinetics of bSiO₂.

4.3. Effect of Micronutrient Availability on the Silicate Pump

Our results can also be interpreted in view of the factors driving the “silicate pump” as defined by Dugdale et al. [1995] as the preferential export of Si compared to N out of the euphotic zone. Many laboratories and field studies focusing on the effect of Fe limitation on the elemental ratio of diatoms have demonstrated that low Fe availability increases Si:C and Si:N ratios [Marchetti and Cassar, 2009, and references therein]. This suggests that Fe limitation should stimulate the silicate pump. During *P. delicatissima* growth, Fe limitation also increased Si:N by approximately twofold compared to that of replete cells (1.21 ± 0.37 mol mol⁻¹ and 0.63 ± 0.08 mol mol⁻¹, respectively, Table 1). More importantly, Si:N remained higher in the Fe-limited treatment than in the replete treatment during 3 weeks of remineralization (Figure 2), with values close to those measured by Salter et al.

[2007] in sediment traps from the Southern Ocean (from 1.3 ± 0.3 to 11.5 ± 1.2 mol mol⁻¹). Thus, our results support the assumption that Fe-limited cells may export more Si relative to N than replete cells, not only because of the decoupling between Si and N uptake during growth (approximately twofold difference in our case) but also due to the decoupling between Si and N remineralization during dissolution (up to approximately sixfold difference). These observations also support the hypothesis of Brzezinski *et al.* [2002] that Fe fertilization during glacial eras would have not only directly stimulated the organic carbon pump but also increased the ocean inventory of dSi relative to nitrate, due to decreased Si:N in diatoms in the Southern Ocean. According to this hypothesis, a redistribution of the dSi stock throughout the ocean should have favored the growth of diatoms over coccolithophorids, decreased the carbonate counter pump, and increased the depth of remineralization. Our results indicate that Fe fertilization may decrease Si:N not only during growth but also during recycling, which should indeed increase the inventory of dSi relative to nitrate.

On the contrary, Cu limitation did not decrease Si:N of *P. delicatissima* during growth (0.50 ± 0.04 mol mol⁻¹) compared to that of replete cells (0.63 ± 0.08 mol mol⁻¹) (Table 1). However, during the dissolution experiment, Si:N of Cu-limited cells increased to a maximum value which was approximately threefold higher than that of replete cells, with the final result of stimulating the silicate pump. Thus, like Fe limitation, Cu limitation induces a decoupling between Si and N remineralization during dissolution, and that decoupling is more important in driving the silicate pump than the decoupling between Si and N uptake during growth. As Fe and Cu may (co)limit phytoplankton growth in the open ocean [Peers *et al.*, 2005], more studies are obviously needed to determine whether our results remain valid for other limitations and other diatom species. Anyway, these results clearly demonstrate that using the elemental ratio of growing cells may bias the estimation of Si and N export. Indeed, aggregates, which are major contributors to the sedimentation flux, contain live and dead diatoms [Turner, 2002]. The Si:N ratio of exported particles is likely to be in between values measured during cell growth and during remineralization.

4.4. Conclusion and Perspectives

Iron and copper limitations during growth significantly decreased the postmortem dissolution of the marine diatom *Pseudo-nitzschia delicatissima*. This decrease likely resulted from a change in the proportions of two potential bSiO₂ phases within the frustules and from a change in the dissolution constants of these two phases as suggested by previous studies [Gallinari *et al.*, 2002; Moriceau *et al.*, 2009]. To our knowledge, our study is the first to evidence an effect of trace metal limitations during diatom growth on their dissolution kinetics. More studies are obviously needed to determine if our results reflect a general behavior, or are induced by the type of limiting growth conditions, or are species dependent. A better understanding of the mechanisms that influence the dissolution constants would also allow to better parameterize bSiO₂ dissolution in ecosystems models. That would improve their predictions on the amount of bSiO₂ that dissolves within the euphotic zone and the amount of bSiO₂ that is exported to the seafloor.

Our results also partly confirm Boyle's hypothesis [Boyle, 1998]: Fe- (and Cu-) limited cells may export more Si relative to N compared to replete cells and stimulate the silicate pump. However, this may be due to a decoupling between the recycling of Si and N during dissolution, rather than solely driven by the degree of silicification in live cells. This conclusion was not predictable from the measurement of Si:N of live cells, and it encourages caution when extrapolating the elemental ratios measured during growth to the fate of the particles in the water column.

References

- Bidle, K. D., and F. Azam (1999), Accelerated dissolution of diatom silica by marine bacterial assemblages, *Nature*, 397(6719), 508–512.
- Bidle, K. D., and F. Azam (2001), Bacterial control of silicon regeneration from diatom detritus: Significance of bacterial ectohydrolases and species identity, *Limnol. Oceanogr.*, 46(7), 1606–1623.
- Boyd, P., and M. Ellwood (2010), The biogeochemical cycle of iron in the ocean, *Nat. Geosci.*, 3(10), 675–682.
- Boyle, E. (1998), Oceanography—Pumping iron makes thinner diatoms, *Nature*, 393(6687), 733–734.
- Brzezinski, M. A., C. J. Pride, V. M. Franck, D. M. Sigman, J. L. Sarmiento, K. Matsumoto, N. Gruber, G. H. Rau, and K. H. Coale (2002), A switch from Si(OH)₄ to NO₃⁻ depletion in the glacial Southern Ocean, *Geophys. Res. Lett.*, 29(12), 1564, doi:10.1029/2001GL014349.
- Buesseler, K. O., and P. W. Boyd (2009), Shedding light on processes that control particle export and flux attenuation in the twilight zone of the open ocean, *Limnol. Oceanogr.*, 54(4), 1210–1232.
- Claquin, P., V. Martin-Jezequel, J. C. Kromkamp, M. J. W. Veldhuis, and G. W. Kraay (2002), Uncoupling of silicon compared with carbon and nitrogen metabolisms and the role of the cell cycle in continuous cultures of *Thalassiosira pseudonana* (Bacillariophyceae) under light, nitrogen, and phosphorus control, *J. Phycol.*, 38(5), 922–930.

Acknowledgments

The set of PON, bSiO₂, and dSi raw data is available in the supporting information Data Set S1. This work has been funded by the Agence Nationale de la Recherche (ANR) (ICOP: Iron, Copper, and Oceanic Phytoplankton, ANR-10-JCJC-606) and by the EU Framework 7 EuroBASIN project. This work was also supported by the "Laboratoire d'Excellence" Labex MER (ANR-10-LABX-19) and cofunded by a grant from the French government under the program "Investissements d'Avenir." The authors would like to thank four anonymous reviewers for their insightful comments which improved this manuscript. We are grateful to M. Le Goff for her help in nutrient analysis, to A. Masson for PON measurements, and to the PIMM platform of the Université de Brest for the SEM pictures.

- Closset, I., M. Lasbleiz, K. Leblanc, B. Quéguiner, A. J. Cavagna, M. Elskens, J. Navez, and D. Cardinal (2014), Seasonal evolution of net and regenerated silica production around a natural Fe-fertilized area in the Southern Ocean estimated with Si isotopic approaches, *Biogeosciences*, 11(20), 5827–5846.
- Coale, K. H. (1991), Effects of iron, manganese, copper, and zinc enrichments on productivity and biomass in the sub-arctic Pacific, *Limnol. Oceanogr.*, 36(8), 1851–1864.
- de Baar, H. J. W., and J. La Roche (2003), Trace metals in the oceans: Evolution, biology and global change, in *Marine Science Frontiers for Europe*, edited by G. Wefer, F. Lamy, and F. Mantoura, pp. 79–105, Springer, Berlin.
- Dixit, S., P. Van Cappellen, and A. J. van Bennekom (2001), Processes controlling solubility of biogenic silica and pore water build-up of silicic acid in marine sediments, *Mar. Chem.*, 73(3–4), 333–352.
- Dugdale, R. C., F. P. Wilkerson, and H. J. Minas (1995), The role of a silicate pump in driving new production, *Deep Sea Res., Part I*, 42(5), 697–719.
- Frayse, F., O. S. Pokrovsky, J. Schott, and J.-D. Meunier (2009), Surface chemistry and reactivity of plant phytoliths in aqueous solutions, *Chem. Geol.*, 258(3), 197–206.
- Gallinari, M., O. Ragueneau, L. Corrin, D. J. DeMaster, and P. Treguer (2002), The importance of water column processes on the dissolution properties of biogenic silica in deep-sea sediments I. Solubility, *Geochim. Cosmochim. Acta*, 66(15), 2701–2717.
- Gehlen, M., L. Beck, G. Calas, A.-M. Flank, A. Van Bennekom, and J. Van Beusekom (2002), Unraveling the atomic structure of biogenic silica: Evidence of the structural association of Al and Si in diatom frustules, *Geochim. Cosmochim. Acta*, 66(9), 1601–1609.
- Gehlen, M., L. Bopp, N. Ernprin, O. Aumont, C. Heinze, and O. Ragueneau (2006), Reconciling surface ocean productivity, export fluxes and sediment composition in a global biogeochemical ocean model, *Biogeosciences*, 3(4), 521–537.
- Geider, R. J., and J. La Roche (2002), Redfield revisited: Variability of C: N: P in marine microalgae and its biochemical basis, *Eur. J. Phycol.*, 37(1), 1–17.
- Gnanadesikan, A. (1999), A global model of silicon cycling: Sensitivity to eddy parameterization and dissolution, *Global Biogeochem. Cycles*, 13(1), 199–220.
- Gómez, F., H. Claustre, P. Raimbault, and S. Souissi (2007), Two high-nutrient low-chlorophyll phytoplankton assemblages: The tropical central Pacific and the offshore Perú-Chile Current, *Biogeosciences*, 4(6), 1101–1113.
- Gordon, L. I., J. C. Jennings Jr., A. A. Ross, and J. M. Krest (1993), *A Suggested Protocol for Continuous Flow Automated Analysis of Seawater Nutrients (Phosphate, Nitrate, Nitrite and Silicic Acid) in the WOCE Hydrographic Program and the Joint Global Ocean Fluxes Study*, Technical Report Rep. 93–1, pp. 1–55, Chemical Oceanography Group, Oregon State Univ., College of Oceanography, Corvallis, Oreg.
- Greenwood, J. E., V. W. Truesdale, and A. R. Rendell (2001), Biogenic silica dissolution in seawater—In vitro chemical kinetics, *Prog. Oceanogr.*, 48(1), 1–23.
- Hilborn, R., and M. Mangel (1997), *The Ecological Detective: Confronting Models With Data*, 314 pp., Princeton Univ. Press, Princeton, N. J.
- Hurd, D. C., and K. Takahashi (1983), On the estimation of minimum mechanical loss during an in situ biogenic silica dissolution experiment, *Mar. Micropaleontol.*, 7(5), 441–447.
- Hurd, D. C., and S. Birdwhistell (1983), On producing a more general model for biogenic silica dissolution, *Am. J. Sci.*, 283(1), 1–28.
- Kamatani, A. (1982), Dissolution rates of silica from diatoms decomposing at various temperatures, *Mar. Biol.*, 68(1), 91–96.
- Kamatani, A., and J. P. Riley (1979), Rate of dissolution of diatom silica walls in seawater, *Mar. Biol.*, 55(1), 29–35.
- Le Grand, F., A. Lelong, M. Long, H. Hegaret, E. Bucciarelli, and P. Soudant (2015), Lipid composition modifications of the marine diatom *Pseudo-nitzschia delicatissima* under copper starvation, *Eur. J. Phycol.*, 50(1), 39–39.
- Lelong, A., H. Hegaret, and P. Soudant (2011), Cell-based measurements to assess physiological status of *Pseudo-nitzschia* multiseria, a toxic diatom, *Res. Microbiol.*, 162(9), 969–981.
- Lelong, A., E. Bucciarelli, H. Hégarret, and P. Soudant (2013), Iron and copper limitations differently affect growth rates and photosynthetic and physiological parameters of the marine diatom *Pseudo-nitzschia delicatissima*, *Limnol. Oceanogr.*, 58(2), 613–623.
- Leynaert, A., E. Bucciarelli, P. Claquin, R. C. Dugdale, V. Martin-Jezequel, P. Pondaven, and O. Ragueneau (2004), Effect of iron deficiency on diatom cell size and silicic acid uptake kinetics, *Limnol. Oceanogr.*, 49(4), 1134–1143.
- Loucaides, S., P. Van Cappellen, V. Roubex, B. Moriceau, and O. Ragueneau (2011), Controls on the recycling and preservation of biogenic silica from biomineralization to burial, *Silicon*, 4(1), 7–22.
- Maldonado, M. T., A. E. Allen, J. S. Chong, K. Lin, D. Leus, N. Karpenko, and S. L. Harris (2006), Copper-dependent iron transport in coastal and oceanic diatoms, *Limnol. Oceanogr.*, 51(4), 1729–1743.
- Marchetti, A., and N. Cassar (2009), Diatom elemental and morphological changes in response to iron limitation: A brief review with potential paleoceanographic applications, *Geobiology*, 7(4), 419–431.
- Mongin, M., D. M. Nelson, P. Pondaven, and P. Tréguer (2006), Simulation of upper-ocean biogeochemistry with a flexible-composition phytoplankton model: C, N and Si cycling and Fe limitation in the Southern Ocean, *Deep Sea Res., Part II*, 53(5), 601–619.
- Moriceau, B., M. Garvey, U. Passow, and O. Ragueneau (2007), Evidence for reduced biogenic silica dissolution rates in diatom aggregates, *Mar. Ecol. Prog. Ser.*, 333, 129–142.
- Moriceau, B., M. Goutx, C. Guigue, C. Lee, R. Armstrong, M. Duflos, C. Tamburini, B. Charrière, and O. Ragueneau (2009), Si–C interactions during degradation of the diatom *Skeletonema marinoi*, *Deep Sea Res., Part II*, 56(18), 1381–1395.
- Mullin, J., and J. Riley (1965), The spectrophotometric determination of silicate-silicon in natural waters with special reference to sea water, *Anal. Chim. Acta*, 46, 491–501.
- Nelson, D. M., and J. J. Goering (1977), Near-surface silica dissolution in the upwelling region off northwest Africa, *Deep Sea Res.*, 24(1), 65–73.
- Nelson, D. M., and M. A. Brzezinski (1997), Diatom growth and productivity in an oligotrophic midocean gyre: A 3-yr record from the Sargasso Sea near Bermuda, *Limnol. Oceanogr.*, 42(3), 473–486.
- Nelson, D. M., P. Treguer, M. A. Brzezinski, A. Leynaert, and B. Queguiner (1995), Production and dissolution of biogenic silica in the ocean—Revised global estimates, comparison with regional data and relationship to biogenic sedimentation, *Global Biogeochem. Cycles*, 9(3), 359–372.
- Passow, U., M. A. French, and M. Robert (2011), Biological controls on dissolution of diatom frustules during their descent to the deep ocean: Lessons learned from controlled laboratory experiments, *Deep Sea Res., Part I*, 58(12), 1147–1157.
- Peers, G., and N. M. Price (2006), Copper-containing plastocyanin used for electron transport by an oceanic diatom, *Nature*, 441(7091), 341–344.
- Peers, G., S. A. Quesnel, and N. M. Price (2005), Copper requirements for iron acquisition and growth of coastal and oceanic diatoms, *Limnol. Oceanogr.*, 50(4), 1149–1158.
- Pichevin, L. E., R. S. Ganeshram, W. Geibert, R. Thunell, and R. Hinton (2014), Silica burial enhanced by iron limitation in oceanic upwelling margins, *Nat. Geosci.*, 7(7), 541–546.

- Ploug, H., and U. Passow (2007), Direct measurement of diffusivity within diatom aggregates containing transparent exopolymer particles, *Limnol. Oceanogr.*, *52*(1), 1–6.
- Pondaven, P., C. Fravallo, D. Ruiz-Pino, P. Treguer, B. Queguiner, and C. Jeandel (1998), Modelling the silica pump in the Permanently Open Ocean Zone of the Southern Ocean, *J. Mar. Syst.*, *17*(1–4), 587–619.
- Price, N. M., G. I. Harrison, J. G. Hering, R. J. Hudson, P. M. V. Nirel, B. Palenik, and F. M. M. Morel (1988–1989), Preparation and chemistry of the artificial algal culture medium Aquil, *Biol. Oceanogr.*, *6*, 443–461.
- Queguiner, B. (2013), Iron fertilization and the structure of planktonic communities in high nutrient regions of the Southern Ocean, *Deep Sea Res., Part II*, *90*, 43–54.
- Ragueneau, O., and P. Tréguer (1994), Determination of biogenic silica in coastal waters: Applicability and limits of the alkaline digestion method, *Mar. Chem.*, *45*(1–2), 43–51.
- Ragueneau, O., et al. (2000), A review of the Si cycle in the modern ocean: Recent progress and missing gaps in the application of biogenic opal as a paleoproductivity proxy, *Global Planet. Change*, *26*(4), 317–365.
- Rickert, D., M. Schluter, and K. Wallmann (2002), Dissolution kinetics of biogenic silica from the water column to the sediments, *Geochim. Cosmochim. Acta*, *66*(3), 439–455.
- Roubeix, V., S. Becquevort, and C. Lancelot (2008), Influence of bacteria and salinity on diatom biogenic silica dissolution in estuarine systems, *Biogeochemistry*, *88*(1), 47–62.
- Salter, I., R. S. Lampitt, R. Sanders, A. Poulton, A. E. S. Kemp, B. Boorman, K. Saw, and R. Pearce (2007), Estimating carbon, silica and diatom export from a naturally fertilised phytoplankton bloom in the Southern Ocean using PELAGRA: A novel drifting sediment trap, *Deep Sea Res., Part II*, *54*(18–20), 2233–2259.
- Schultes, S., C. Lambert, P. Pondaven, R. Corvaisier, S. Jansen, and O. Ragueneau (2010), Recycling and uptake of Si(OH)₄ when Protozoan grazers feed on diatoms, *Protist*, *161*(2), 288–303.
- Sunda, W. G., N. M. Price, and F. M. Morel (2005), Trace metal ion buffers and their use in culture studies, in *Algal Culturing Techniques*, edited by R. Anderson, pp. 35–63, Academic Press, Burlington.
- Tréguer, P., and P. Le Corre (1975), *Manuel D'analyse Des Sels Nutritifs Dans L'eau de Mer (utilisation de l'autoanalyseur II Technicon)*, 2nd ed., Université de Bretagne Occidentale, Brest.
- Tréguer, P., D. M. Nelson, A. J. Vanbennekom, D. J. Demaster, A. Leynaert, and B. Queguiner (1995), The silica balance in the world ocean—A reestimate, *Science*, *268*(5209), 375–379.
- Trick, C. G., B. D. Bill, W. P. Cochlan, M. L. Wells, V. L. Trainer, and L. D. Pickell (2010), Iron enrichment stimulates toxic diatom production in high-nitrate, low-chlorophyll areas, *Proc. Natl. Acad. Sci. U.S.A.*, *107*(13), 5887–5892.
- Truesdale, V. W., J. E. Greenwood, and A. R. Rendell (2005a), In vitro, batch-dissolution of biogenic silica in seawater—The application of recent modelling to real data, *Prog. Oceanogr.*, *66*(1), 1–24.
- Truesdale, V. W., J. E. Greenwood, and A. Rendell (2005b), The rate-equation for biogenic silica dissolution in seawater—New hypotheses, *Aquat. Geochem.*, *11*(3), 319–343.
- Turner, J. T. (2002), Zooplankton fecal pellets, marine snow and sinking phytoplankton blooms, *Aquat. Microb. Ecol.*, *27*(1), 57–102.
- Van Cappellen, P. (1996), Reactive surface area control of the dissolution kinetics of biogenic silica in deep-sea sediments, *Chem. Geol.*, *132*(1–4), 125–130.
- Van Cappellen, P., S. Dixit, and J. van Beusekom (2002), Biogenic silica dissolution in the oceans: Reconciling experimental and field-based dissolution rates, *Global Biogeochem. Cycles*, *16*(4), 1075, doi:10.1029/2001GB001431.

Erratum

In the originally published version of this article, the acknowledgments section contained incomplete funding information. This error has since been corrected, and this version may be considered the authoritative version of record.